

# Borehole radar for environment study

Motoyuki Sato  
Tohoku University, Sendai, Japan

**Abstract:** Borehole radar is one kind of GPR, but it can be used in deep boreholes, and it has many advantages compared with low frequency borehole EM tools, and surface GPR. We have developed various techniques on borehole radar for environment study. The hardware development includes broadband radar system with the functions of polarimetry and interferometry. By using these systems, we tested the measurements to applications such as subsurface fracture characterization, subsurface cavity detections. In this paper, we will describe the advantages of the advanced radar technology for environment studies, and show some experiment results.

## 1. Introduction

A new geophysical exploration technique is always a key issue for better understanding and usage of subsurface. In a very complex geological situation, and dense surface conditions which are typical in Korea and Japan, high frequency electromagnetic techniques including Ground Penetrating Radar (GPR) is quite useful due to its high resolution. Compared to other techniques such as seismic, GPR can be applied in a small area without undesirable effects from the surroundings.

We have developed borehole radar techniques, and applied to many engineering applications. Borehole radar has been used in many deep subsurface applications, but it is always suffered from relatively short penetrating depth. In order to overcome the disadvantages of the borehole radar, we have proposed new techniques, namely polarimetry and interferometry. Also, under the Japan-Korea research collaboration agreement, we have conducted several borehole radar measurements in Korea. In this paper, we introduce the potential of borehole radar in geophysics and geophysical exploration and engineering applications.

## 2. Cross-Hole Borehole Radar Measurement

We have developed a stepped frequency borehole radar system and have tested in many fields (Sato and Miwa, 2000), (Miwa et al., 1999). The frequency bandwidth of the system is quite wide, and it can operate between 1MHz up to 500MHz. The downhole probe is also flexible in the arrangement and it can be used both for single-hole measurement and cross-hole measurement. When multiple boreholes are available around a subsurface target, cross-hole radar measurement is one of the most powerful survey arrangements. We have conducted field experiment of cross-hole borehole radar measurement in Korea in October 2000. The purpose of this field test is acquisition of borehole radar data by single-hole and cross-hole measurement, where the radar target is an air-filled cavity. Especially, our interest is the performance of the stepped frequency radar for detecting the fractures and the cavity, and its capability of imaging by radar polarimetry.

### Data acquisition

The host rock was granite. Fig.1 shows the plan view of the test site. B-1, B-2 and B-3 indicate the borehole numbers, which we used for measurement. For the single-hole measurement, we used B-3 borehole. And for the cross-hole measurement, the transmitter was set in B-2 or in B-3 borehole and the receiver was set in B-1 borehole.

The frequency-domain data was acquired at 201 points between 2MHz and 402MHz by using a vector network analyzer. The acquired data is Fourier transformed and the time-domain signal can be obtained.

Single-Hole Reflection Measurement is the most common borehole radar measurement technique, where a transmitter and a receiver is moved together in a single. Reflections from a cavity and natural fractures can be directly imaged. Moving average subtraction processing was used to remove the strong direct coupling signal between the transmitter and the receiver and enhance the reflection. Fig.2(a) shows the single-hole reflection by dipole-dipole antennas combination, after averaged signal is subtracted. Reflections from natural fractures appear at 78m and 92m from the moving averaged radar profile. Reflection from a cavity could not be detected in this radar profile.

Fig. 2(b) shows the radar profile by cross-hole radar measurement. The transmitter and the receiver was kept at the same depth, and moved simultaneously. Anomalous arrival time due to the cavity clearly appears at 77-83m. This is due to faster wave propagation through an air-filled cavity. We think this phenomenon is very important and we are now modelling the wave propagation in this condition.

Cross-Hole Fan measurement, where a transmitter was set at one depth and the receiver was moved in another borehole. This data set was acquired for tomography analysis. The raw data is not easy to interpret, however, the cavity was also clearly detected by fast arriving signal.

By using the phase delay along a path in cross-hole measurement, we estimate the relative permittivity of the host rock is 5.5 – 6.0.

### Cavity Detection

Tomography analysis is a common signal processing procedure for cross-hole radar and seismic measurement. It can estimate the absolute value of dielectric constant from the information of arrival time between two holes. However, the drawback of the tomography approach is its low resolution and stability. When we apply tomography, we have to assume grids to be estimated, but its size is restricted by the number of measurement paths between two boreholes and computation time. Also, if we assume too fine grids, the estimation becomes unstable. On the contrary, migration approach is much stable, although it cannot estimate the absolute value of the material. We have found that when the host rock is relatively homogeneous, migration technique can be very effectively applied to GPR data set, too. Fig.3 shows the reconstructed image of a cavity by reverse time migration technique.

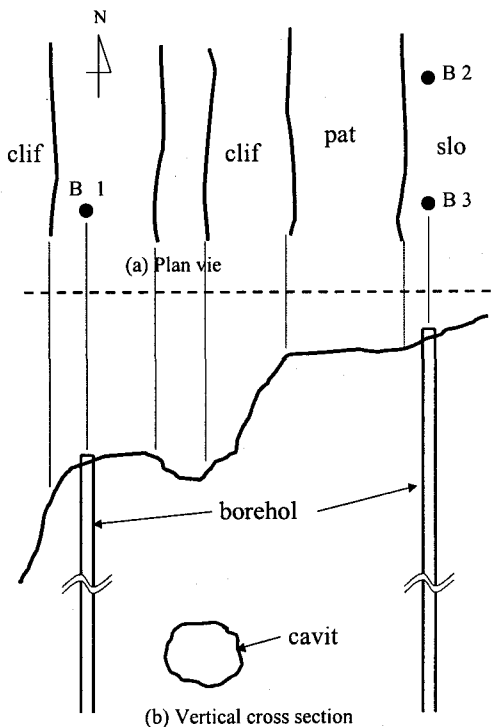
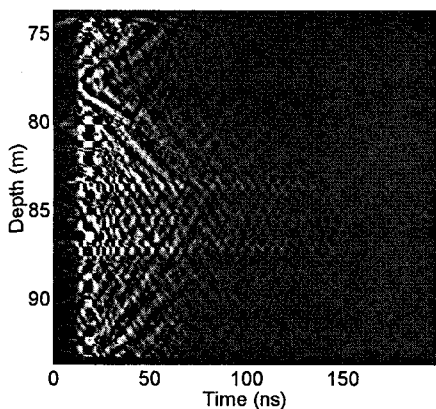
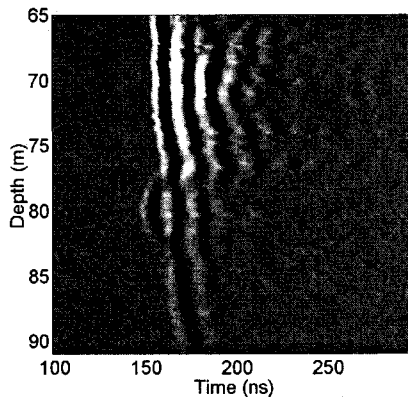


Fig. 1. Borehole location in the test site.



(a) Single-hole



(b) Cross-hole

Fig. 2. Borehole radar raw data for a cavity detection.

### 3. Interferometric Borehole Radar

When the radar resolution has limitation, we can use interferometric approach in order to obtain higher resolution image. Radar interferometry is a new radar technology which was often applied to Synthetic Aperture Radar (SAR)

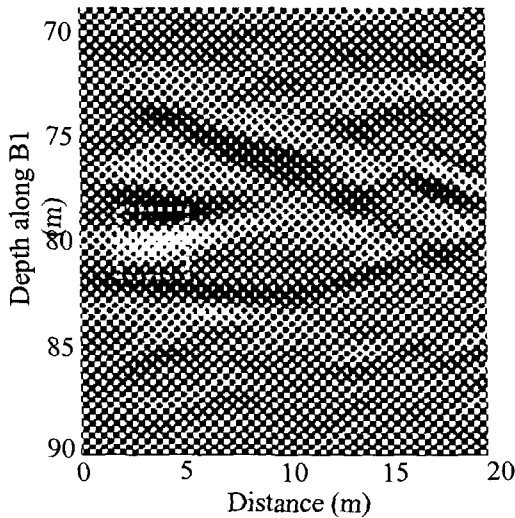


Fig. 3. Reconstructed image of a cavity.

acquired by space craft. However, the same principle can be used if we use two receivers instead of one receiver in borehole radar.

### Radar system

The system for borehole interferometry is not very different from the conventional borehole radar system, except it has two receivers. Fig. 4 shows the system diagram of the developed borehole radar system. A vector network analyzer put on the ground generates RF signals. These signals are transmitted to R/O (RF signal to optical signal) converter and converted to optical signals. Then the optical signals are transmitted through a single mode optical fiber and converted to RF signals at an O/R (optical signal to RF signal) converter installed in the transmitting antenna element, and the RF signals are radiated from the transmitting antenna. The signals received by two receiving antennas are transmitted through the analog optical link and received by the vector network analyzer. A RF switch is connected in front of receiving port of the vector network analyzer and selects signals received by the receiver #1 or #2.

The analog optical link is used in interferometric borehole radar system to isolate the antennas electrically from any other parts of the radar system, which achieves an ideal antenna radiation pattern, and it works at the frequency range from 2 to 500 MHz. It consists of one downlink and two uplinks. The down-hole parts of the each links have the size of 25 mm in diameter and 180 mm in length and can be installed in antenna elements. They are smaller than our conventional one (Sato et. al., 1995; Sato and Miwa, 2000).

### Field measurement

Field measurements for testing the interferometric borehole radar system were carried out in Korea, November 2001. This test site is quarry mine and its host rock is granite. There are five vertical boreholes with the diameter of 75 mm (NX-size) in this site and four of them are filled with groundwater up to a few meters in depth. Various geophysical explorations were carried out in this test site including resistivity logging and borehole televiewer by KIGAM (Korea Institute of Geology, Mining & Materials). By these measurements, it is already known that there are some vertical fractures in this test site.

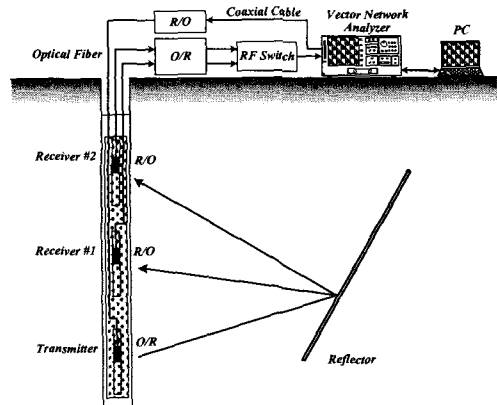


Fig. 4 . System diagram of interferometric borehole radar system.

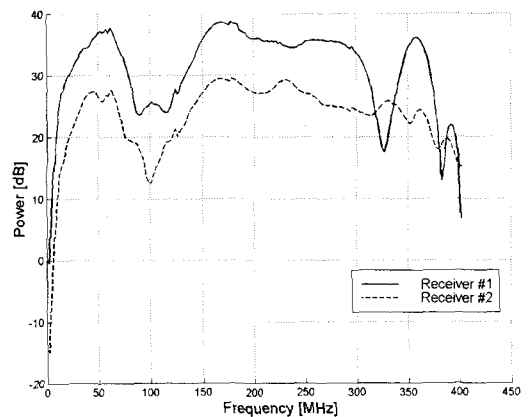


Fig. 5. Power spectra of the received signal at 25 m in depth (BH-2, Iksan).

In these measurements, the dipole antennas were used as a transmitter and receivers. These antennas have the size of 35 mm in diameter and 900 mm in length. The antenna elements are made of hollow brass cylinders. These antennas were installed in a hollow plastic cylinder having a diameter of 42 mm for insulation from water in a borehole. The radar system acquired the data in frequency domain at frequency range of 2 to 402 MHz. The antenna separation between the transmitter and the receiver #1 was 1.6 m and #2 was 2.6 m. Under these parameters, single-hole measurements were carried out.

The power spectra of the two signals received by receiver #1 and #2 at depth of 25 m in BH-2 are shown in Fig.5. The difference of the power can be observed and it is approximately 10 dB. It includes the attenuation by surrounding medium and spherical spreading of the EM wave. The raw radar profiles received by the receiver #1 is shown in Fig.6(a). From this figure, we can estimate the surrounding medium around this borehole is almost homogeneous

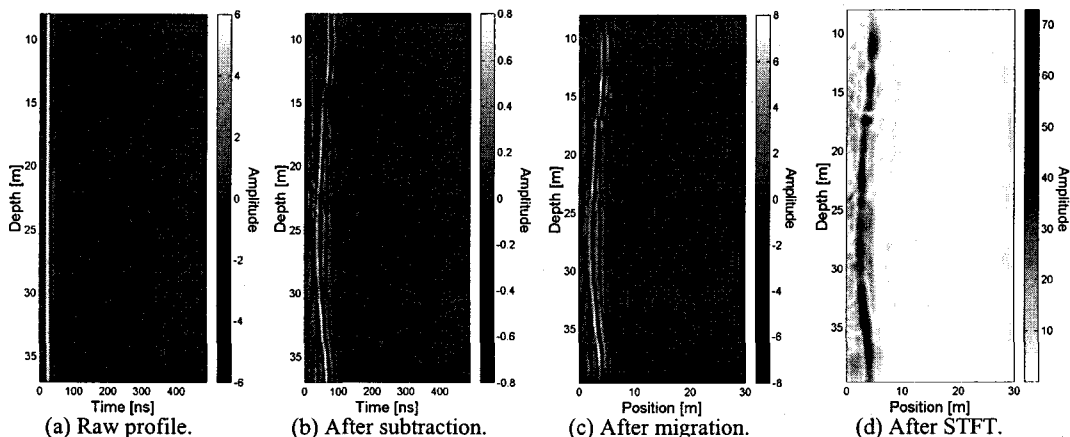


Fig. 6. Raw radar profile and processed images (receiver #1, BH-2, Iksan).

### Signal processing

The direct coupling signals can be observed strongly at about 20 ns in Fig.6(a). The direct coupling component can be reduced by subtraction of the averaged signal from the original signal. This is a typical signal processing technique in single-hole measurements of borehole radar. Fig.6(b) shows the radar profile after subtraction of the all-depth-averaged signal. Vertical fractures can be seen clearly by reduction of the direct coupling components.

Migration is a technique, which reconstructs an image from a radar profile by inversely tracing the time in the wave propagation process. Here, diffraction stacking method is used as a kind of migration method. In this technique, the transformation from the radar profile in time domain obtained by the measurement  $i_m(t, z_r)$  to the image in spatial domain  $i(x, z)$  is represented by

$$i(x, z) = \int i_m(\tau, z_r) dz_r \tag{1}$$

where

$$\tau = \frac{\sqrt{x^2 + (z - z_r)^2}}{v} \tag{2}$$

and  $v$  is the velocity of electromagnetic wave. This processing is equivalent to synthetic aperture processing in space borne SAR, because, the images after processing this technique are projected to real geographical coordinate system and the resolution can be improved. The migrated image of receiver #1 using this technique is shown in Fig.6(c).

STFT is used to extract the phase with position information from the image after migration. STFT using the windowing function  $h(x)$  is represented by

$$s(x, \omega) = \int i(x')h(x - x')e^{-j\omega x'} dx' \tag{3}$$

This processing is applied to each depth of the migrated image. Fig.6(d) shows the amplitude image after processing STFT at spatial frequency of  $0.7 \text{ m}^{-1}$  using the Gaussian function as a windowing function and this windowing function is already optimized for this dataset. Spatial frequency of  $0.7 \text{ m}^{-1}$  is equivalent to around 80 MHz in granite when velocity of EM wave is assumed, and 80 MHz is dominant frequency of this radar system.

As for the structure of the data, this image is equivalent to a SAR image, because, the single frequency component can be extracted by this processing. Therefore, the phase at each position can be obtained from this dataset, and the phase difference images between receiver #1 and #2 at spatial frequency of  $0.7 \text{ m}^{-1}$  is shown in Fig. 7. If we take simply the phase difference of two SAR images, the phase information contains the  $2\pi$  ambiguity. There-

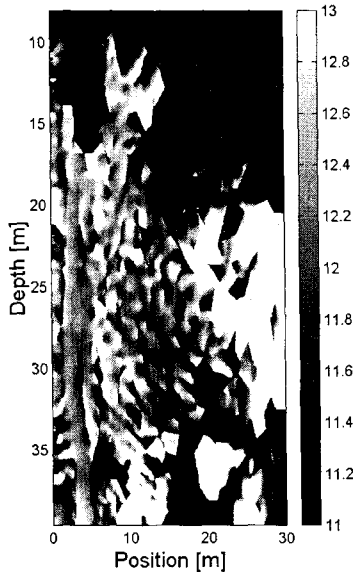


Fig. 7. Phase difference.

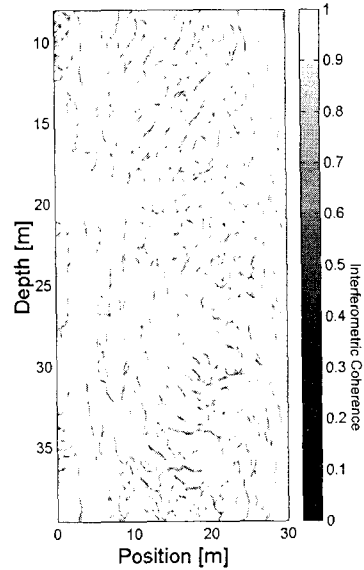


Fig. 8. Interferometric coherence at spatial frequency of  $0.7 \text{ m}^{-1}$  (BH-2, Iksan).

fore, this image needs to be unwrapped by phase unwrapping. Fig. 7 shows the phase image after processing Goldstein algorithm for phase unwrapping (Goldstein et al, 1988).

The important factor in an interferometric image is a correlation between two images. It depends on the quality of the phase and is degraded by any amount of noise. The quality can be evaluated by calculation of interferometric coherence. Interferometric coherence  $\gamma$  for interferometric images is defined as the absolute value of the normalized complex cross-correlation between two images (Cloude and Papathanassiou, 1998).

$$\gamma \equiv \frac{|\langle s_1 s_2^* \rangle|}{\sqrt{\langle s_1 s_1^* \rangle \langle s_2 s_2^* \rangle}} \quad (6)$$

where the operator  $\langle \rangle$  is an expectation operator. The interferometric coherence  $\gamma$  takes between 0 and 1. If the two images are identical, it becomes 1 and if the two images do not correlate, it becomes 0. The interferometric coherence of the two images after processing STFT at spatial frequency of  $0.7 \text{ m}^{-1}$  is shown in Fig.8. In this calculation, the expectation operators were replaced by spatial averaging in 3 by 3 pixels. The average value of the interferometric coherence in whole image is 0.96 and these images have relatively high coherence.

#### 4. Conclusions

Borehole radar was applied for detection and identification of air-filled cavity. Polarimetric single-hole and cross-hole data was acquired. The cavity could be detected by the raw data of time-domain cross-hole radar profile. The result is consistent with the conventional single frequency detection technique using a double-dip attenuation profile. Then the new interferometric borehole radar was tested in granite quarry and its characteristics were evaluated.

Test sites suitable for scientific research are sometimes very difficult to find. However, measurements in good sites could be achieved by the Japan-Korea collaborative research. Also the field measurement was very smooth, because the both organizations have the similar but very high technical potential, therefore we could solve many practical problems for data acquisition very easily.

## Acknowledgements

We thank to Prof. Jung-Woong Ra of KAIST (currently with KJIST) and colleagues of KIGAM for providing the test site and their cooperation in the field measurement. This work was supported by JSPS Grant-In-Aid Scientific Research (S) 14102024, and also it was supported by the Japan-Korea Basic Scientific Cooperation Program.

## References

- Choi H. and Ra, J., 1999, Detection and Identification of a Tunnel by Iterative Inversion from Cross-Borehole CW Measurements, *Microwave and Optical Technology Letters*, vol.21, no.6, 458-465.
- Cloude, S. R. and Papathanassiou, K. P., 1998, "Polarimetric SAR Interferometry," *IEEE Trans. Geosci. Remote Sensing*, Vol. 36, No. 5, pp. 1551-1565.
- Goldstein, R. M., Zebker, H. A. and Werner, C. L., 1988, "Satellite radar interferometry: Two-dimensional phase unwrapping," *Radio Science*, Vol. 23, No. 4, pp. 713-720.
- Liu, S. and Sato, M., 2002, Electromagnetic Logging Technique Based on Borehole Radar, *IEEE Trans. Geoscience & Remote Sensing*, vol.40, no.9, September, 2002, 2083-2092.
- Miwa, T., Sato, M. and Niitsuma, H., 1999, Subsurface Fracture Measurement with Polarimetric Borehole Radar, *IEEE Trans. Geoscience & Remote Sensing*, vol.37, no.2, 828-837.
- Park, S. Choi, H. and Ra, J., 1998, Underground Tomogram from Cross-Borehole Measurements, *Microwave and Optical Technology Letters*, vol.18, no.6, 402-406.
- Ra, J., Choi, H. and Park, S., 1998, Underground Tomogram Constructed from In-Situ Cross-Borehole Measurements, *Proc. KJJC*, 255-258.
- Sato, M. and Miwa, T., 2000, Polarimetric Borehole Radar System for Fracture Measurement, *Subsurface Sensing Technologies and Applications*, vol.1, no.1, 161-175.
- Sato, M., Miwa, T. and Niitsuma, H., 1995, "Application of polarimetric borehole radar to crack characterization," *Trans. SPWLA 36th Annual Logging Symposium*, pp. FFF1-FFF12.
- Sato, M. and Miwa, T., 2000, "Polarimetric borehole radar system for fracture measurement," *Subsurface Sensing Tech. and Appl.*, 1, pp. 161-175.
- Takahashi, K., Liu, S. and Sato, M., 2002, "Interferometric borehole radar system," in *Proc. 9th Int. Conference on Ground Penetrating Radar 2002*, pp. 19-24.
- Takahashi, K., Kim, J. -H. and Sato, M., 2003, "Estimation of subsurface structure by borehole radar system using radar interferometry," in *Proc. The 6th SEGJ Int. Symposium -Imaging technology-*, pp. 466-471.